

ALBERT-LUDWIGS-UNIVERSITÄT FREIBURG
ADVANCED PHYSICS LAB COURSE
SUMMER SEMESTER 2022

EXPERIMENT ON 27.-28.09.2022

Laser-Gyroscope

Group 13:
30.09.2022

Assistant:

Abstract

In the laser gyroscope experiment the fundamental functionality of a laser gyroscope is examined. The major goals are to calibrate the optics as well as to find the lock-in threshold and the instrument scale factor of the setup. Additionally, a measurement to check the angular velocity of the turntable was conducted. The first part of the experiment focuses on the calibration whereas the second part evaluates the angular velocity as well as the lock-in threshold and the instrument scale factor.

In the first part a good calibration with low-noise signals has been achieved. Afterwards an exact value for the lock-in threshold could not be determined, but it is considered to be between 1 deg s^{-1} and 1.4 deg s^{-1} . The value for the instrument scale factor has been determined to be $6610 \pm 40 \text{ Hz deg}^{-1}$, which lies within a 1σ -environment of the value given in the instruction of the laser gyroscope.

Contents

| | | |
|----------|--|-----------|
| 1 | Introduction | 4 |
| 2 | Theory | 4 |
| 2.1 | Table of the used variables | 4 |
| 2.2 | Basic Theory of Light | 4 |
| 2.3 | The Sagnac effect | 5 |
| 2.4 | Characteristics of the used Laser gyroscope | 5 |
| 2.4.1 | HeNe-Laser | 6 |
| 2.4.2 | Laser modes and etalon | 6 |
| 2.4.3 | Ring Laser Gyroscope | 7 |
| 2.4.4 | Lock-in-effect | 7 |
| 2.4.5 | Measuring method | 8 |
| 3 | Setup and measurements | 9 |
| 4 | Data analysis and discussion of uncertainties | 11 |
| 4.1 | Calibration of the laser gyroscope | 11 |
| 4.2 | Determination of the angular velocity of the turntable | 12 |
| 4.3 | Finding the lock-in threshold | 14 |
| 4.4 | Finding the instrument scale factor | 15 |
| 5 | Summary and discussion of the results | 18 |
| 5.1 | Summary of the results | 18 |
| 5.2 | Comparison with expectation | 18 |
| 5.3 | Discussion of results and uncertainties | 19 |
| 6 | Bibliography | 20 |
| 7 | Appendix | 21 |
| 7.1 | Tables and graphics | 21 |
| 7.2 | Measurement of the angular rotation | 22 |
| 7.3 | Measurement of the instrument scale factor | 24 |
| 7.4 | Lab notes | 25 |

List of Tables

| | | |
|---|---|----|
| 1 | Used symbols for the parameters used in the protocol. | 4 |
| 2 | Comparison with the expectation | 18 |
| 3 | Measured angular velocities for clockwise and counter-clockwise rotations | 21 |
| 4 | Fit parameters and χ^2 -values for the instrument scale factor measurements. . . . | 21 |

List of Figures

| | | |
|----|--|----|
| 1 | Setup used by Sagnac | 5 |
| 2 | Energy level diagram of the HeNe-Laser | 6 |
| 3 | Modes of the HeNe-Laser | 7 |
| 4 | Expectation of the measurement considering the lock-in effect | 8 |
| 5 | Setup for the analysis of the beat frequency and conversion to the TTL-Signal . . | 8 |
| 6 | Pictures of the turntable with the laser turned off and on | 9 |
| 7 | Close-up pictures of the setup | 9 |
| 8 | Setup for the experiment | 10 |
| 9 | Calibration of the beat frequency detector | 11 |
| 10 | Oscilloscope Screenshots of the signal for different angular velocities | 12 |
| 11 | measurement of the angular velocity for setting 10 | 13 |
| 12 | Linear regression to find the conversion factor between setup and angular velocity | 14 |
| 13 | Measurement 1 of the beat frequency | 15 |
| 14 | Mean of the beat frequency | 16 |
| 15 | Measurement of the angular velocity for setting 1 | 22 |
| 16 | Measurement of the angular velocity for setting 1.2 | 22 |
| 17 | Measurement of the angular velocity for setting 1.4 | 22 |
| 18 | Measurement of the angular velocity for setting 1.6 | 22 |
| 19 | Measurement of the angular velocity for setting 1.8 | 22 |
| 20 | Measurement of the angular velocity for setting 2 | 22 |
| 21 | Measurement of the angular velocity for setting 3 | 23 |
| 22 | Measurement of the angular velocity for setting 4 | 23 |
| 23 | Measurement of the angular velocity for setting 6 | 23 |
| 24 | Measurement of the angular velocity for setting 8 | 23 |
| 25 | Measurement 2 of the beat frequency | 24 |
| 26 | Measurement 3 of the beat frequency | 24 |
| 27 | Lab notes - page 1 | 25 |
| 28 | Lab notes - page 2 | 26 |
| 29 | Lab notes - page 3 | 27 |

1 Introduction

The laser-gyroscope-experiment focuses on the preparation of a laser gyroscope made out of a HeNe-Laser with a triangular mirror arrangement on a rotatory plate. The main goal is to measure the instrument scale factor of the gyroscope, represented by the slope of the linear relation between beat-frequency of the gyroscope and angular velocity of the rotation-plate. In addition, a comparison between the angular velocity given by the manufacturer and the actual angular velocity is performed using the `phyphox`-app. In a last step a range for the lock-in-threshold can be found.

Gyroscopes and especially laser gyroscopes have many different applications [1]. A main application is the navigation, with gyroscopes being used in vehicles, aircrafts and ships. Another application is the accurate pointing. In physical research, gyroscopes are widely spread. Earlier, they were used to get the earth rotation and to prove Einsteins theory of relativity. Nowadays they are for example used to detect gravitational waves.

2 Theory

The following sections introducing the theory and methodology necessary for the experiment are mainly based on the experiment description, which is provided by the advanced physics lab team [1], the theoretical description by Dr Walter Luhs [2] and the manual for the laser gyroscope [3].

2.1 Table of the used variables

Tab. 1: Used symbols for the parameters used in the protocol.

| Symbol | Parameter |
|----------------------------|--|
| $f_{(\text{beat/cw/ccw})}$ | (beat/clockwise/counter-clockwise) frequency |
| Δf | difference in frequencies |
| λ | wavelength |
| $\Delta\phi$ | phase shift |
| c | speed of light |
| ϵ | dielectric factor |
| E | electric field |
| I | Intensity |
| ω | angular velocity |
| v | velocity |
| r | distance from rotation centre |
| A | area (surrounded by the beams) |
| d | length of the resonator |
| Ω_{lock} | lock-in-threshold |

2.2 Basic Theory of Light

The laser gyroscope is a special gyroscope using laser light to measure rotational velocities. Light can be described as electro-magnetic radiation with the magnetic field always perpendicular to the electric field. The intensity I of light is thereby proportional to the square of the amplitude $|\vec{E}|$ [2]:

$$I = \frac{c\epsilon}{4\pi} |\vec{E}|^2. \quad (1)$$

c is the speed of light and ϵ the corresponding dielectric factor. Other important characteristics of light are the wavelength λ , the frequency f , the propagation direction and the polarisation (linear, circular, elliptical). Another effect that is relevant for the laser gyroscope is interference, which means the superposition of different waves. In this experiment interference is used to get the difference between the frequencies of the two beams travelling clockwise f_{cw} and counter-clockwise f_{ccw} , which is also known as the beat-frequency f_{beat} [2]:

$$f_{beat} = f_{cw} - f_{ccw}. \quad (2)$$

The phenomenon of two waves with very close frequency interfering is called beat. It is characterised by one frequency being the average of the two original frequencies and another frequency – the beat-frequency – that provides an enveloping wave which varies the amplitude. By measuring this beat-frequency later the angular velocity can be found.

2.3 The Sagnac effect

The Sagnac effect is based on the fact that processes behave differently in rotating systems. The effect is the basis for the ring interferometer. Two beams of light are split in a beam splitter and then propagate in different directions, one clockwise and one counter-clockwise before being reunited. When the ground starts rotating with the angular velocity ω , a phase shift $\Delta\phi$ occurs that can be described by the following formula derived by Sagnac [2]:

$$\Delta\phi = \frac{8\pi}{\lambda c} \omega A. \quad (3)$$

A represents the area enclosed by the two beams. Therefore the phase shift is proportional to the angular velocity and can also be used to find rotations [2]. In Figure 1 the original setup used by Sagnac can be found.

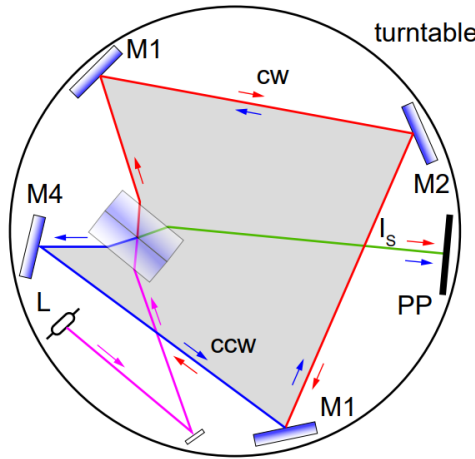


Fig. 1: Original setup of an interferometer used by Sagnac. The beam emitted by the lamp (pink) is sent to a beam splitter which splits the beam in clockwise (red) and counter-clockwise (blue) directions. The beam is reunited (green) and detected by a photosensitive screen. The setup is built on a turntable. The graphic is taken from [2], p. 7.

2.4 Characteristics of the used Laser gyroscope

The used laser gyroscope is realised by a HeNe-Laser with $\lambda = 632.8 \text{ nm}$ and three mirrors arranged in a triangular setup on a turning table. In this section the most important characteristics of the used components are introduced.

2.4.1 HeNe-Laser

For the used laser, as the active medium a Helium-Neon-Gas is used. As required, this laser has an inversion between two energy levels. By electron collisions, the helium is excited into the semi-stable states 2^1S_0 and 2^3S_1 and then transfers energy to the neon atoms which are excited into $3s$ and $2s$ states. By mainly emitting the laser light of $\lambda = 632.8 \text{ nm}$ the neon de-excites into the $2p$ state. In a last step it goes back to the $1s$ state by spontaneous emission and to the ground state by wall collisions. The whole energy level diagram can be found in [Figure 2](#).

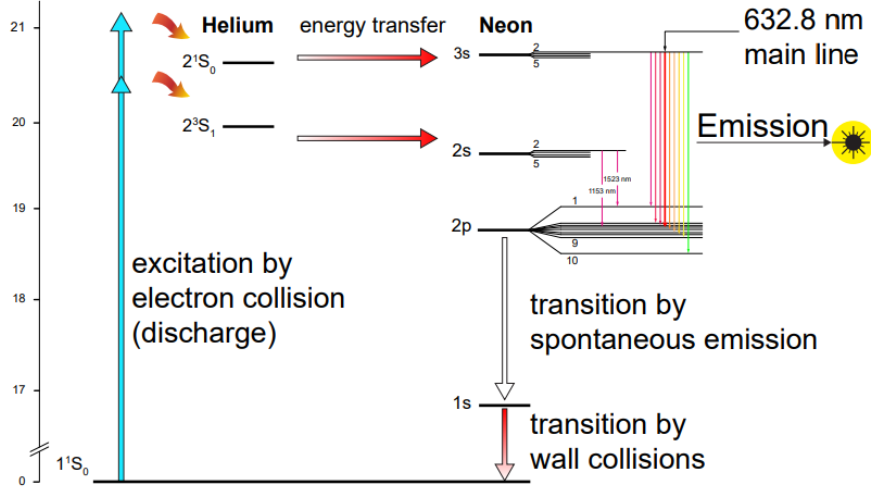


Fig. 2: Energy level diagram of the HeNe-Laser. On the left site the excitation of the helium is portrayed whereas on the right side the de-excitation of the neon and the emission of the laser light are shown. The graphic is taken from [2], p. 10.

To guarantee the optical stability of the laser, two flat and one curved mirror with its focal point on the opposite side of the triangle are used. By optical stability it is meant, that after any number of passes the ray diameter still is smaller than the mirror diameter [2].

2.4.2 Laser modes and etalon

In a resonator theoretically infinite modes are possible by taking all the standing waves where a half of the wavelength λ is a multiple n of the resonator length d :

$$\frac{n\lambda}{2} = \frac{nc}{2f} = d. \quad (4)$$

Therefore all the modes with a difference in frequency of $\Delta f = c/(2d)$ are possible. For the HeNe-Laser there are a couple of modes that fit under the respective Gain-Profile. This effect can be seen in [Figure 3](#). By adding etalon to the setup, which is a ground and polished glass cylinder, a filtering of the modes can be done and only one mode remains stable. The etalon profile is also portrayed in [Figure 3](#).

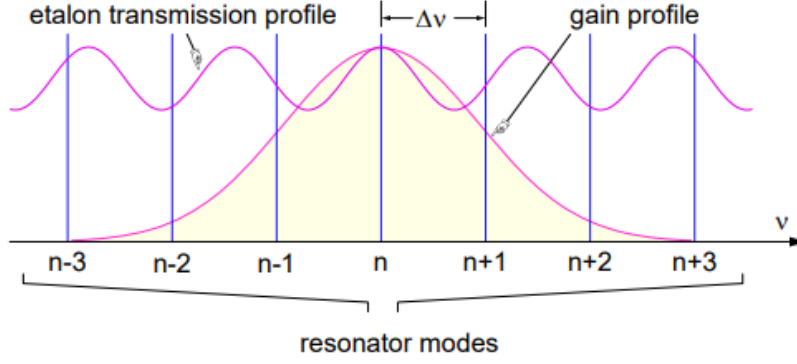


Fig. 3: Sketch of the modes of the HeNe-Laser with its gain profile added in pink and the etalon transmission profile added in purple. The graphic is taken from [2], p. 13.

2.4.3 Ring Laser Gyroscope

In the Ring Laser Gyroscope the relativistic Doppler effect for light is used. For the frequency $f_{+/-}$ of the light travelling in the direction of the rotation (+) and against this direction (−) we get [2]:

$$f_{+/-} = f_0 \left(1 \pm \frac{v}{c} \pm \frac{r\omega}{c} \right). \quad (5)$$

f_0 is the ground frequency, c the speed of light, v the moving velocity, r the distance from the rotation axis and ω the angular velocity. For the difference in frequency due to the rotation we therefore get [2]:

$$\Delta f_{\text{rot}} = \frac{4F}{L\lambda} \omega, \quad (6)$$

$$F = \pi r^2, \quad (7)$$

$$L = 2\pi r. \quad (8)$$

2.4.4 Lock-in-effect

A last important effect that has to be discussed is the lock-in-effect. It occurs for slow angular velocities where the difference in frequency is small. For those velocities a coupling occurs that leads to no frequency difference being measurable. Due to scattering of the mirrors, the intensities of the different modes interact with each other leading to a non-measurable frequency difference. The angular velocity that marks the border of the lock-in-effect is called the lock-in-threshold Ω_{lock} . For the measurement this means that for small values of the rotation frequencies the expected linear relation between beat frequency and rotation rate is broken as shown in Figure 4.

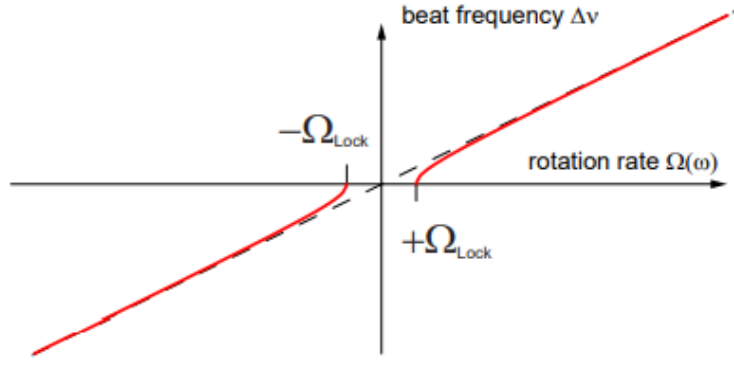


Fig. 4: Sketch of the expected linear curve with the rotation rate on the x -axis and the beat frequency on the y -axis. In addition the lock in effect and the lock-in-threshold Ω_{lock} are portrayed. The graphic is taken from [2], p. 14.

2.4.5 Measuring method

For the measurement, the beat frequency is found by reuniting the clockwise and counter-clockwise beams and splitting them up again to be able to measure with two photo-diodes with a phase shift of exactly 180° to each other. By having both signals, the frequency can be easily found by converting the signal in a TTL-signal with every change between zero and one being at the crossing points of the two signals. This signal can then be analysed much easier and a counting rate leading to a frequency can be found. In Figure 5a the setup for the beam-analysis is visible and in Figure 5b the conversion from measured signal to TTL-signal is sketched.

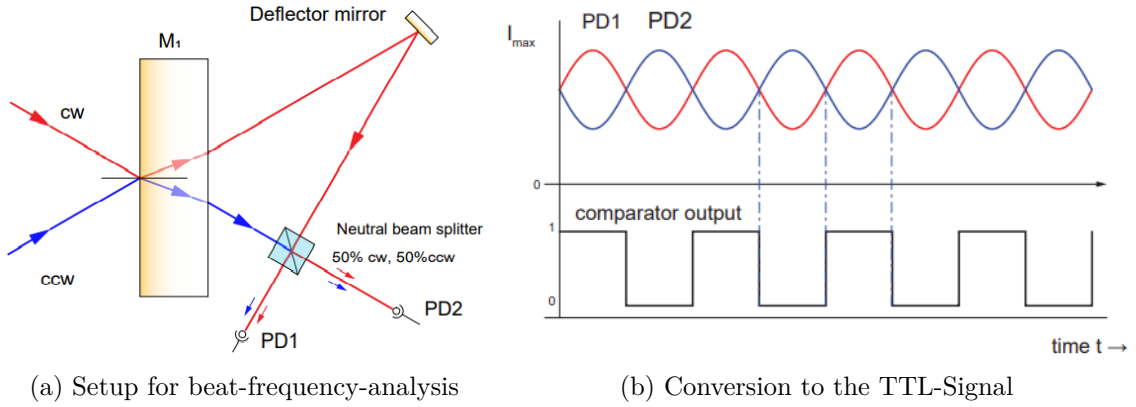


Fig. 5: In the first graphic the setup for the beam analysis is portrayed with the clockwise (red) and counter-clockwise (blue) beam. The red beam is reflected in the deflector mirror. Both beams meet in the beam splitter and are directly splitted again for analysis with the Photo-Diode 1 (PD1) and 2 (PD2). The second graphic shows the conversion of the two signals from the diode to a TTL-signal, that can be used to get the counting rate and therefore the frequency.

3 Setup and measurements

The setup used for performing the measurements can be split in two parts. First the turntable with the optics on it and then the electronics.

The optics on the turntable consist of the HeNe-laser, which sends laser beams in both directions, mirror 1 on the left side of the laser-tube and mirror 2 on the right side of it. Both mirrors are flat. There is also a third mirror, which is concave and placed in a way to form a triangle with the other two mirrors. The focal point of the mirror lays on the opposite site of the triangle. In addition, there is a mount with etalon in it, placed in the optical path of the laser between mirror 1 and mirror 3. Behind mirror 3 a deflection mirror and a beam splitter are added in order to overlay both laser beams for the measurement with the photodiodes.

The turntable with the laser turned off and the laser turned on can be found in [Figure 6](#).

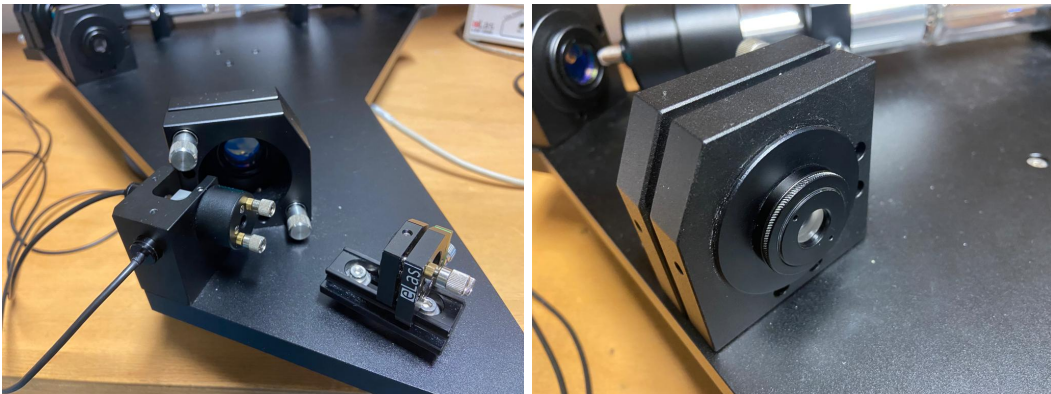


(a) Turntable with turned off laser

(b) Turntable with turned on laser

Fig. 6: In the left picture one can see the turntable with the laser turned off. In the right picture the turntable with the turned on laser is displayed.

Close-up pictures of the back-side of mirror 3 with a deflection mirror on the right side of it, a beam splitter and the two photodiodes as well as the etalon in the mount can be found in [Figure 7a](#) and [Figure 7b](#).



(a) Mirror 3 with a deflection mirror, a beam splitter and two photodiodes

(b) Etalon in a mount between Mirror 1 and Mirror 3

Fig. 7: In the left picture one can see the back of mirror 3 in the centre, a deflection mirror on the right side and a beam splitter next to the two photodiodes. In the right picture the etalon, which is mounted in the optical path between mirror 1 and mirror 3, is displayed.

The electronics needed for the measurement are the following. First of all a voltage generator to operate the laser is connected. The used settings are a current of 6.5 mA and an amplifier gain of 0.01. There are also two photodiodes, which are placed in different distances to the beam splitter to ensure a phase shift of 180° between them. These diodes are connected to an oscilloscope. As mentioned in the theory part, the resulting TTL-signal is analysed by the frequency counter. There is also a motor connected to the turntable to rotate the optics in both directions with an adjustable speed. The described setup is displayed in [Figure 8](#).

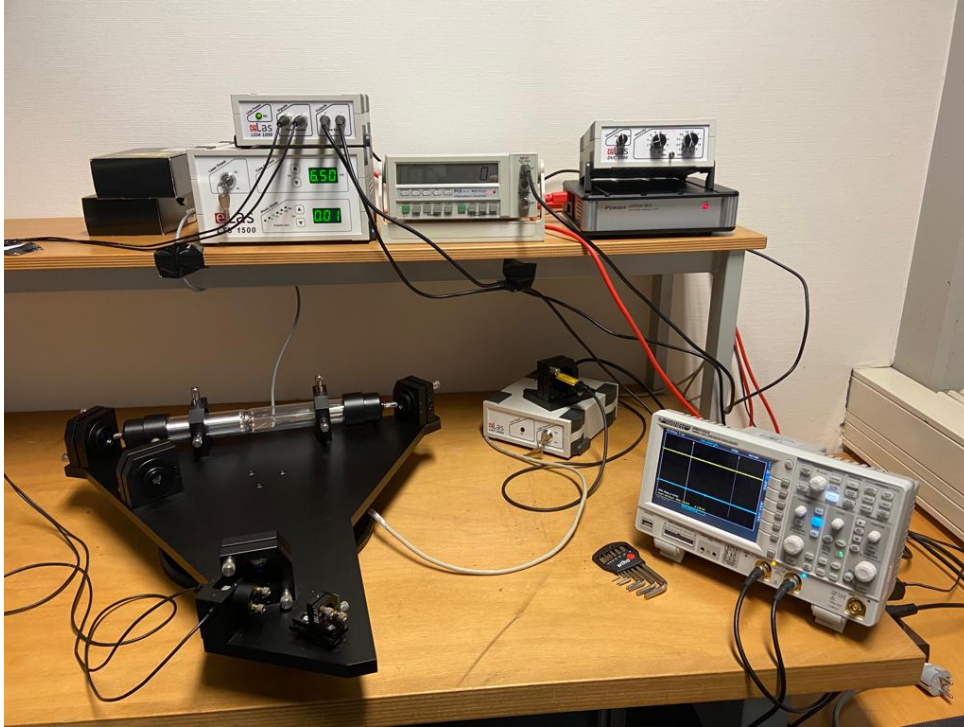


Fig. 8: Setup for the experiment with the electronics and the laser gyro-scope.

The actual calibration process for the laser gyroscope and the adjustment of the mirrors will be described in the following section.

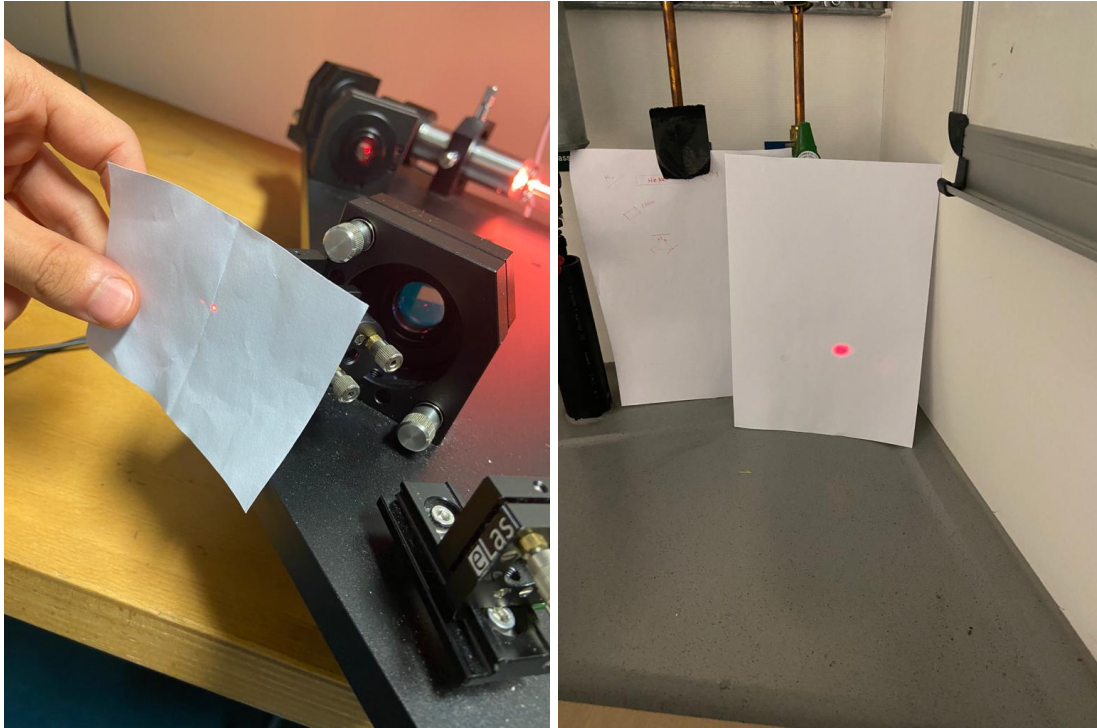
4 Data analysis and discussion of uncertainties

4.1 Calibration of the laser gyroscope

In theory, the first and longest taking part of the experiment is the calibration of the used laser gyroscope. There are several parameters that must be calibrated before performing measurements. A green adjustment laser can be used to find the best setup for the mirrors and optical components. In a first step the position of the HeNe-Tube and the first mirror are adjusted to get a clear signal. Then the second and the third mirror are aligned to get a closed circuit. A good alignment is necessary to get the laser working. In a last step the etalon is aligned before starting the laser.

Because the laser was already working and providing good measurement signals, this part of the alignment could be skipped. The etalon had to be realigned some times during the measurement when the signal got lost. After realigning the etalon, the signal of the laser was again controlled with the oscilloscope.

In a last step, the beat frequency detector had to be aligned by adjusting the deflection mirror and the beam splitter. Therefore the second diode is removed and the superposition is checked directly in front of the detector and at a distance of a few meters as portrayed in [Figure 9](#).



(a) Calibration behind the detector

(b) Calibration at a distance of a few meters

Fig. 9: Calibration of the beat frequency detector: On the left, the signal is observed directly on the position of the second photo diode, on the right, the signal is observed at a distance of a few meters. For both measurements the beams are directly on top of each other.

To check the calibrated setup, the signal of the two diodes is observed on the oscilloscope. A phase shift of exactly 180° should be observed. For small angular velocities a smaller beat frequency should be found and for higher velocities the beat frequency should also get higher. In [Figure 10](#) four different observations with the oscilloscope are presented. For all the signals a clear phase shift is recognisable.

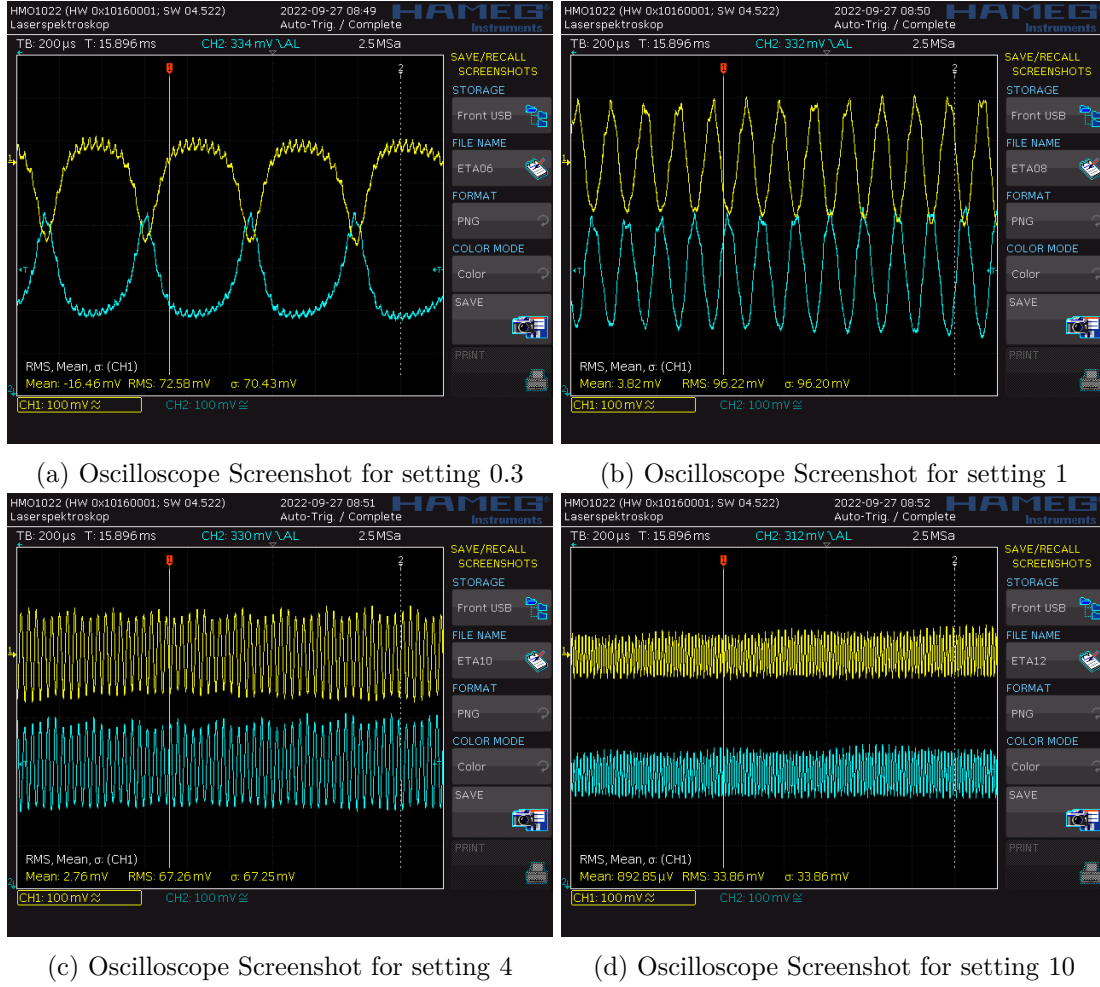


Fig. 10: Four different screenshots of the oscilloscope with the signal of the first diode in channel one and the signal of the second diode in channel two. On the y -axis the voltage measured with the diodes is plotted against the time on the x -axis. The used speeds vary from the setting 0.3 to the setting 10. All the measurements are taken in counter-clockwise-direction.

4.2 Determination of the angular velocity of the turntable

For the angular velocity of the turn table, the values are set with a rotary knob with different setup possibilities in unknown units. To get the right angular velocity in degree per second, the actual rotary speed is measured and compared to the used setup value. Therefore the gyroscope of the *phyphox*-App is used [4]. For different rotation speed setups the actual speed is measured and the data is exported. In the data two plateaus for clockwise and counter-clockwise motion can be found. The angular velocity for the rotation for each setting can be determined by finding the mean of the angular velocity during the rotation with the standard deviation of the mean as its uncertainty [5]. This method is chosen, because it is expected that the angular velocity is constant during the rotation. The limits of the plateaus are set by hand to guarantee that only realistic data point are taken. An exemplary measurement for setting 10 can be found in Figure 11.

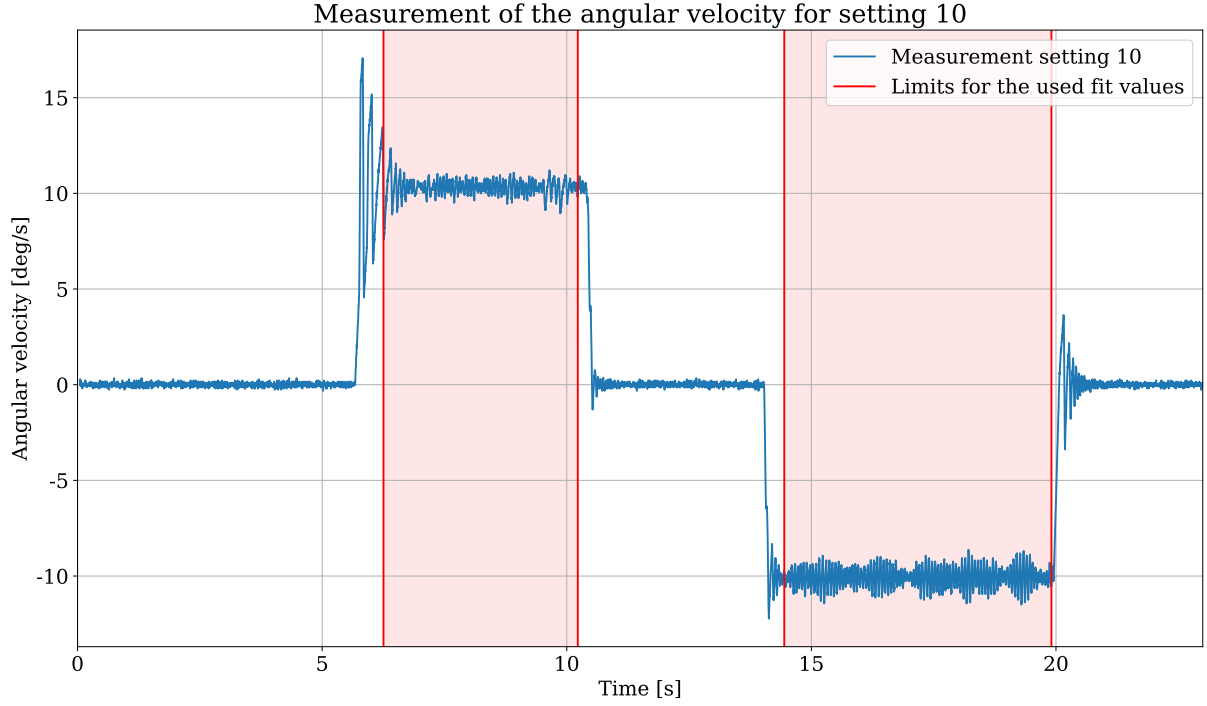


Fig. 11: Measured data with the **phyphox-App-Gyroscope** with the turntable set to an angular velocity of 10. The angular velocity ω in deg/s is plotted against the time t of the measurement in s. In red the limits for the used data are given. The positive plateau represents the clockwise and the negative the counter-clockwise motion.

From the data for the clockwise and counter-clockwise angular velocity we get:

$$\begin{aligned}\omega_{\text{cw}} &= 10.299 \pm 0.012 \text{ deg s}^{-1}, \\ \omega_{\text{ccw}} &= -10.082 \pm 0.012 \text{ deg s}^{-1}.\end{aligned}$$

The measurements for the other settings can be found in the appendix in [Figure 15](#) to [Figure 24](#) and their respective angular velocities in [Table 3](#). Afterwards a linear regression of all the angular velocities is performed in order to find the conversion factor between the actual angular velocity and the setting of the motor. Therefore the measured velocities are plotted against the setting velocities and a linear fit is performed using `scipy.optimize.curve_fit` [6]. The curve fit is performed without regarding the uncertainties of the values due to the uncertainties being extremely small. The uncertainties will also be discussed in [subsection 5.3](#). The measured velocities are plotted together with the linear regression in [Figure 12](#).

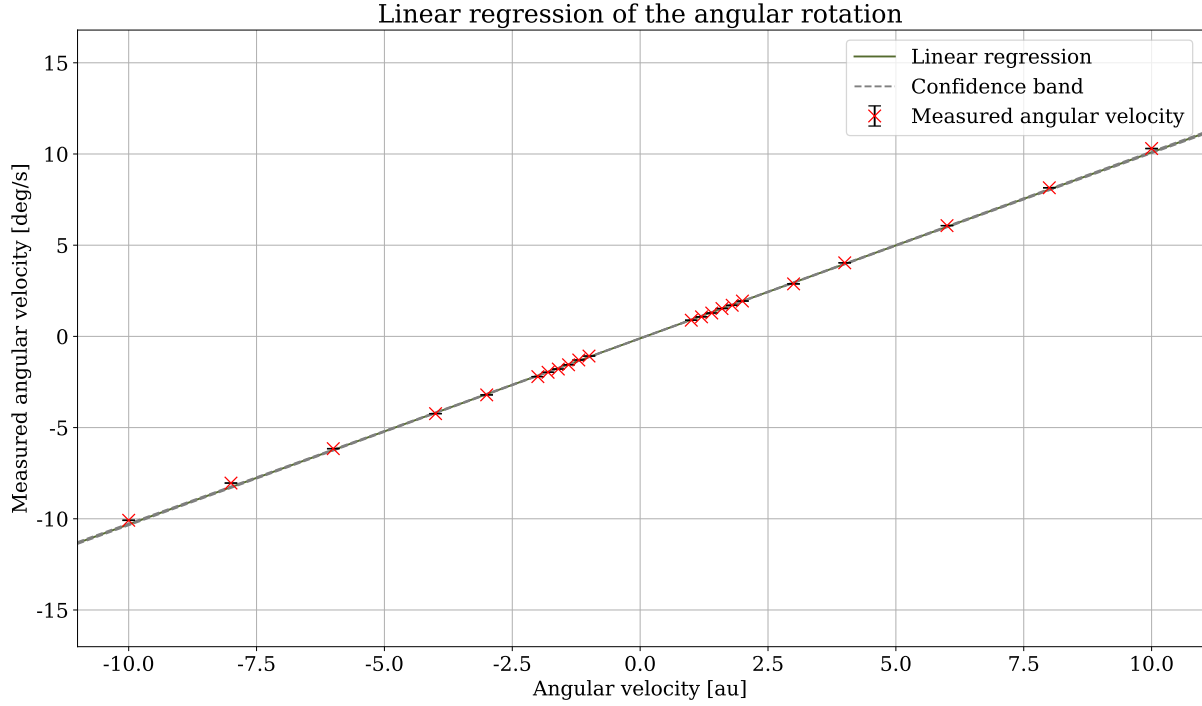


Fig. 12: Linear regression to find the conversion factor between setup and angular velocity. On the y -axis the measured values for the angular velocity ω in deg/s are plotted against the set angular velocity in arbitrary units. In addition to the regression a confidence band is added which is too small to be visible.

The resulting parameters A and B and their covariance $\text{Cov}(A, B)$ are:

$$\begin{aligned} A &= 1.020 \pm 0.005 \text{ deg s}^{-1}, \\ B &= -0.110 \pm 0.012 \text{ deg s}^{-1}, \\ \text{Cov}(A, B) &= 1.8 \times 10^{-6} \text{ deg}^2/\text{s}^2. \end{aligned}$$

The parameters can later be used to convert the setting values into angular velocities. As expected, the velocity conversion-factor A is nearly one, which means that the set value almost corresponds with the angular velocity.

4.3 Finding the lock-in threshold

The lock-in threshold, which is the lower bound of values that contribute to a linear relation between beat frequency and angular velocity, can be estimated by observing the frequency counter and the signal of the photo diodes on the oscilloscope. For small rotational velocities only small frequencies can be observed and high fluctuations appear. Only velocities of the setting 1.4 and higher provide a completely stable signal, thus the lock-in threshold is estimated to be between 1 and 1.4 deg/s. Values below this threshold will later be ignored when discussing the linearity of the relation between beat frequency and angular velocity.

4.4 Finding the instrument scale factor

To find the instrument scale factor as described in [3], which is the slope of the linear relation between beat frequency and angular velocity, for different settings of the angular velocities the beat frequencies are counted. In a first step, all the set velocities ω_{set} need to be converted to the actual angular velocities ω_{real} by using the calibrating measurements from subsection 4.2:

$$\omega_{\text{real}} = A\omega_{\text{set}} + B. \quad (9)$$

The uncertainties are found by using Gaussian propagation of uncertainty, also considering the covariance $\text{Cov}(A, B)$ of the two parameters A and B [7]:

$$\Delta\omega_{\text{real}} = \sqrt{(\omega_{\text{set}}\Delta A)^2 + (\Delta B)^2 + 2\omega_{\text{set}}\text{Cov}(A, B)}. \quad (10)$$

The measured beat frequencies f can now be plotted against the angular velocities and a linear regression with `scipy.optimize.curve_fit` [6] can be performed. As already mentioned, the values with a angular velocity of under 1.4 deg/s are ignored when performing the regression. In Figure 13 the regression for a first measurement is presented.

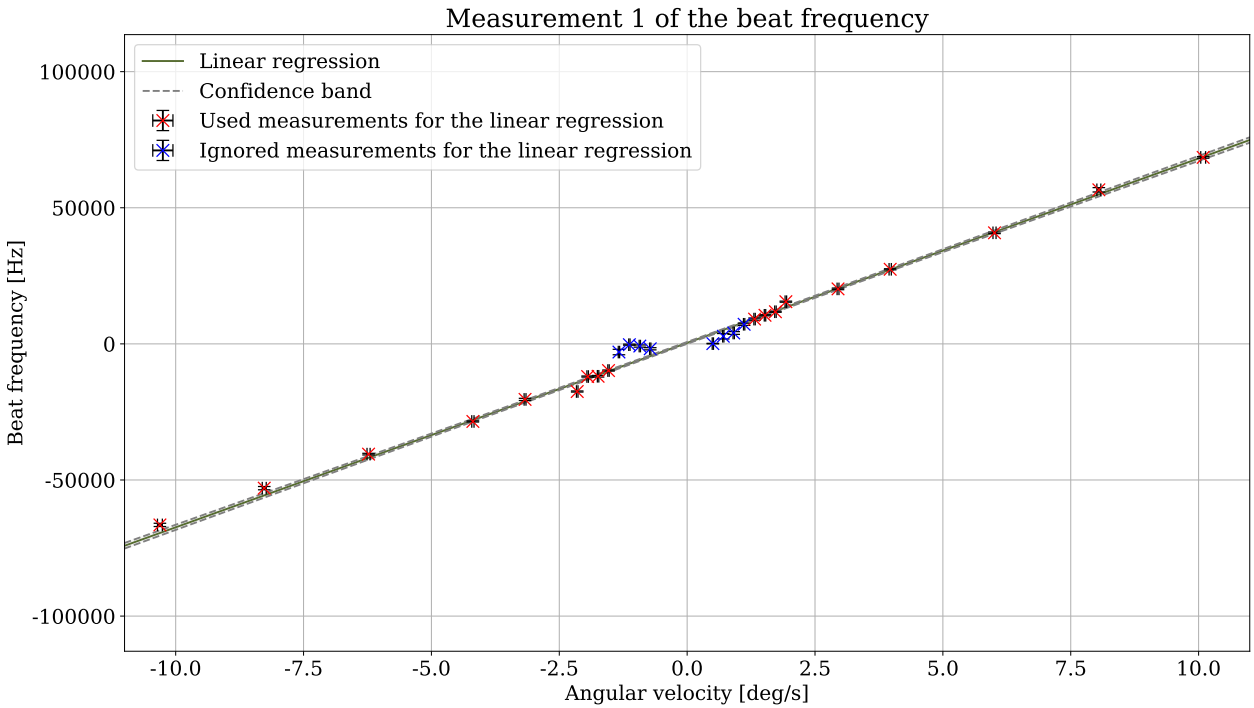


Fig. 13: First measurement of the beat frequencies. On the y -axis the measured values of the beat frequency f in Hz are plotted against the angular velocities ω_{real} in deg/s . In red all the used values for the regression are plotted, in blue the ignored values are shown. The confidence band is again very small.

For the fit parameters the following values are calculated:

$$\begin{aligned} a &= (6780 \pm 90) \text{ Hz s deg}^{-1}, \\ b &= (400 \pm 300) \text{ Hz}. \end{aligned}$$

The slope a of the plot corresponds with the searched instrument scale factor. As a degree for the quality of the fit, a χ^2 -value is calculated [7]. A χ^2 -value of $\chi^2 \approx n - f$ where n is the number of data points and f is the number of fit parameters – in our case 2 – characterises a good fit. If $\chi^2 \gg n - f$, the fit is not a good match for the data [7]. The resulting χ^2 -value is:

$$\chi^2 = 627.$$

With $n - f = 16$ the χ^2 -value does not indicate a good match between the values and the linear fit. Possible reasons for this high value will be discussed in [subsection 5.3](#).

To get a higher accuracy for the instrument scale factor, two additional measurements are performed. The other measurements with their respective linear regression can be found in [Figure 25](#) and [Figure 26](#) in the appendix. The fit parameters as well as the χ^2 -value are concluded in [Table 4](#) in the appendix. To get a final value for the instrument scale factor, for all the angular velocities the measured beat frequencies are averaged [5] to perform another linear regression. The uncertainty is split in a statistical uncertainty derived from the standard deviation of the mean [5] and a systematical uncertainty that comes from the uncertainty of the measurements and the fluctuations on the frequency counter. The systematical uncertainty is again calculated by Gaussian propagation of uncertainties [5]. In [Figure 14](#) the linear regression for the mean of all measurements is displayed together with the linear regression performed with `scipy.optimize.curve_fit` [6].

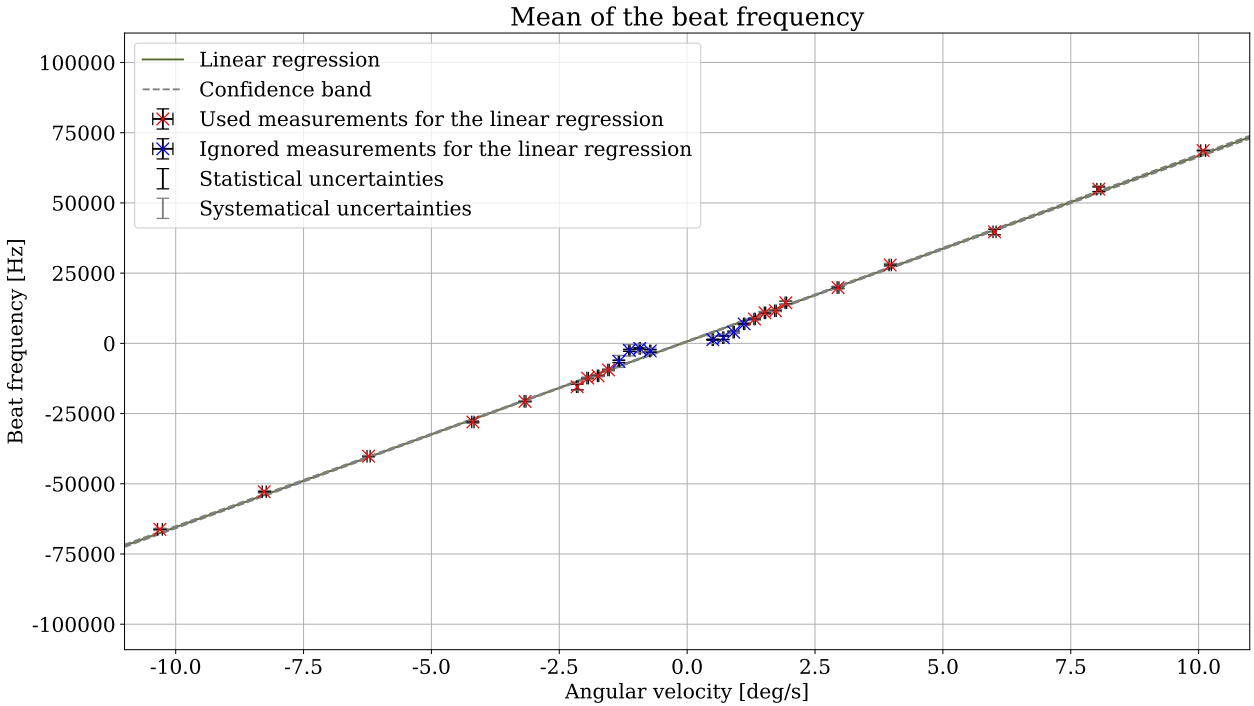


Fig. 14: Linear regression for the mean of the beat frequencies. On the y -axis the averaged values of the beat frequency f in Hz are plotted against the angular velocities ω_{real} in deg/s. In red all the used values for the regression are plotted, in blue the ignored values are shown. The confidence band is very small. For the statistical uncertainties black error bars are used, whereas for systematical uncertainties grey error bars are plotted.

The resulting fit parameters are the following, with a being again the instrument scale factor:

$$\begin{aligned}a &= (6610 \pm 40) \text{ Hz s deg}^{-1}, \\b &= (660 \pm 180) \text{ Hz}.\end{aligned}$$

Again a χ^2 -value is calculated to estimate the quality of the plot:

$$\chi^2 = 458.$$

The χ^2 -value is way too high and thus the plot does not match the values properly. This will also be discussed in [subsection 5.3](#).

5 Summary and discussion of the results

5.1 Summary of the results

After the successful optimisation of the already well prepared calibration of the laser gyroscope, the measurement for finding the conversion formula between the setting of the motor and the actual angular velocity has been conducted:

$$\omega_{\text{real}} = A\omega_{\text{set}} + B,$$

with the following values for A and B

$$\begin{aligned} A &= 1.020 \pm 0.005 \text{ deg s}^{-1}, \\ B &= -0.110 \pm 0.012 \text{ deg s}^{-1}. \end{aligned}$$

When evaluating the lock-in threshold, angular velocities of the setting 1.4 and higher provide a completely stable signal, whereas smaller angular velocities lead to unstable signals with large fluctuations. Thus the lock-in threshold is estimated to be between 1 and 1.4 deg/s.

The resulting value for the instrumental scale factor, which has been calculated by a linear regression of the mean values of the three measurements, has been determined to be

$$a = (6610 \pm 40) \text{ Hz s deg}^{-1}.$$

5.2 Comparison with expectation

The value for the instrumental scale factor can also be calculated by using geometrical properties of the laser gyroscope [3]:

$$a = \frac{l}{\sqrt{3}\lambda}. \quad (11)$$

λ is thereby the wavelength of the laser and l the length of one of the sites of the gyroscope. Because no tools were provided to measure the values needed, the specifications given by the manufacturer were used [3]:

$$\begin{aligned} l &= 0.417 \text{ m}, \\ \lambda &= 632.8 \text{ nm}, \\ \Rightarrow a &= (6640 \pm 15) \text{ Hz s deg}^{-1}. \end{aligned}$$

A comparison between the measured values of the instrument scale factor and the value provided by the manufacturer of the laser gyroscope can be done by using a t -value. The t -value is calculated by dividing the difference between measured and real value with the uncertainty of the measured value. A t -value smaller than two corresponds with a good measurement. The t -values for all the measurements of the instrument scale factor, as well as the values and their relative errors, can be found in [Table 2](#).

Tab. 2: The instrument scale factor, its relative error and the t -value of each measurement are concluded in this table.

| Measurement | Instrument scale factor in Hzs deg ⁻¹ | Relative error | t -value |
|-------------|--|----------------|------------|
| 1 | 6780 ± 90 | 1.3% | 1.55 |
| 2 | 6650 ± 40 | 0.6% | 0.28 |
| 3 | 6510 ± 40 | 0.7% | 2.80 |
| Mean | 6610 ± 40 | 0.6% | 0.66 |

Except for measurement 3 all the calculated values are in a 2σ -environment in comparison to the value provided by the manufacturer, even though the relative errors are all at roughly 1%.

5.3 Discussion of results and uncertainties

A first and most important discussion point can be found in the high χ^2 -values for all the linear regressions used to find the instrument scale factors. There are two main reasons that can explain the high incompatibility with the linear fitting model. The first possibility is, that the lock-in-threshold is not estimated properly. It is possible that some of the values already deviate from the linearity that were still used for the linear fit. Even if that is not the case, the values around the threshold still have a small variance from the linear model. As described in [2], only for angular velocities $\omega \gg \Omega_{\text{lock}}$ a linearity should be observable.

Another even more important point is the high underestimation of the used uncertainties. Even though the values show a good linear course and the resulting slopes lead all to very good results, the calculated χ^2 -values are very high. Therefore an underestimation of the uncertainties is the only logical consequence. Estimating the uncertainties by observing the fluctuations on the frequency counter is very difficult, because high fluctuations can appear on the counter, even if the value is quite stable for a long time. In addition, the number on the frequency counter is changing very rapidly which makes reading out the values in principle very difficult. With uncertainties mostly under 1000 Hz, it could have been sensible to at least double the uncertainties when estimating them.

Another uncertainty that makes the measurement more difficult is the high exposure to acoustical and mechanical disturbances. By knocking on the table, the frequency counter could vary by up to 10 000 Hz and even talking during measurements could affect the results. Although during measurement attention was paid to not disturb the measurement, it can not be excluded that these effects have an influence on the measurement. This effect can also explain that even for the table being in rest, some frequencies unequal to zero could be observed.

Another problem that appeared during the experiment were random rapid rotations of the turntable and sometimes wrong turning speeds. Since those effects could be detected easily, the measurements with problems produced by the turntable were just rejected.

Maybe better results could have been produced by checking the calibration parameters and the positions of the mirrors and the etalon once again. But since varying those parameter slightly could lead to the laser stopping to work at all and a very good initial setup was already configured, no big changes in the setup were done before starting with the measurements. Since all the results are in an acceptable range, this procedure seems to be legit.

A small improvement in the measurement could be performed by comparing the measured frequencies to the frequencies shown on the oscilloscope. Thereby the measurement could be controlled more easily and also the estimation of the uncertainty would be better. Another improvement could be a finer range of angular velocities on the turntable. Since the small velocities can not be used for the linear fit, it would be good to also have smaller steps for the higher velocities. By also increasing the length of the wires that limit the rotation angle of the turntable, longer and more precise measurements could be performed and also higher rotation speeds could be used.

References

- [1] Unknown Author: *Advanced Lab Course (FP-I): Laser gyroscope*, (Freiburg im Breisgau: 2020)
- [2] Dr. Walter Luhs: *LM-0600 HeNe Laser Gyroscope*, (Photonik Ingenieurbüro Dr Walter Luhs, 2018)
- [3] eLas: *Laserausbildungssystem CA-1310 Laser-Gyroskop* www.e-las.com, (Buggingen: eLas, 2020)
- [4] Sebastian Staacks: *phyphox - physical phone experiments* <https://phyphox.org/de/home-de/> (accessed on: 28.09.2022)
- [5] Dr. Christof Bartels, Dr. Lukas Bruder, Dr. Thomas Pfohl: *Datenanalyse Teil A - Skript zur Vorlesung am 06.09.2021*, (Freiburg im Breisgau: 2021/22)
- [6] SciPy 1.0 Contributors: *SciPy 1.0: Fundamental Algorithms for Scientific Computing in Python* <https://rdcu.be/b08Wh> (2020, accessed on: 28.09.2022)
- [7] Dr. Christof Bartels, Dr. Lukas Bruder, Dr. Thomas Pfohl: *Datenanalyse Teil B - Skript zur Vorlesung am 28.02.2022*, (Freiburg im Breisgau: 2021/22)

7 Appendix

7.1 Tables and graphics

Tab. 3: The measured angular velocities ω are concluded with the positive values being clockwise rotations of the setup and the negative values being counter-clockwise rotations.

| Setting of the motor | Measured angular velocity in deg |
|----------------------|----------------------------------|
| 10 | 10.299 ± 0.012 |
| 8 | 8.148 ± 0.008 |
| 6 | 6.073 ± 0.005 |
| 4 | 4.034 ± 0.004 |
| 3 | 2.879 ± 0.010 |
| 2 | 1.938 ± 0.006 |
| 1.8 | 1.706 ± 0.004 |
| 1.6 | 1.527 ± 0.008 |
| 1.4 | 1.281 ± 0.004 |
| 1.2 | 1.071 ± 0.003 |
| 1 | 0.887 ± 0.002 |
| −10 | -10.082 ± 0.012 |
| −8 | -8.042 ± 0.008 |
| −6 | -6.156 ± 0.008 |
| −4 | -4.236 ± 0.005 |
| −3 | -3.207 ± 0.005 |
| −2 | -2.206 ± 0.004 |
| −1.8 | -1.968 ± 0.003 |
| −1.6 | -1.791 ± 0.004 |
| −1.4 | -1.557 ± 0.003 |
| −1.2 | -1.293 ± 0.003 |
| −1 | -1.078 ± 0.003 |

Tab. 4: Fit parameters and χ^2 -values for the instrument scale factor measurements.

| Measurement | Slope a in Hzs deg ^{−1} | Intercept b in Hz | χ^2 |
|-------------|------------------------------------|---------------------|----------|
| 1 | 6780 ± 90 | 400 ± 300 | 627 |
| 2 | 6650 ± 40 | 500 ± 150 | 443 |
| 3 | 6510 ± 40 | 700 ± 200 | 532 |
| Mean | 6610 ± 40 | 660 ± 180 | 458 |

7.2 Measurement of the angular rotation

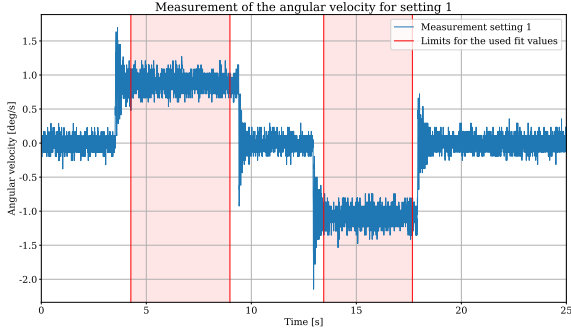


Fig. 15: Measured angular velocity for the clockwise and counter-clockwise rotation for setting 1. The red lines mark the rotation.

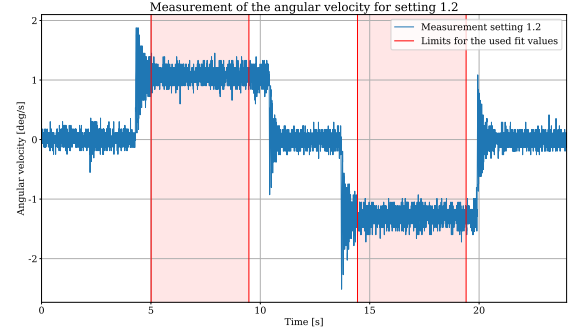


Fig. 16: Measured angular velocity for the clockwise and counter-clockwise rotation for setting 1.2. The red lines mark the rotation.

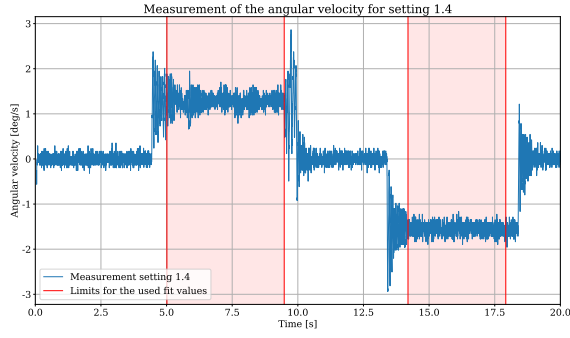


Fig. 17: Measured angular velocity for the clockwise and counter-clockwise rotation for setting 1.4. The red lines mark the rotation.

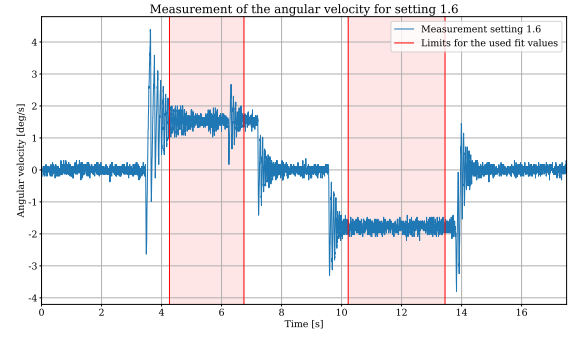


Fig. 18: Measured angular velocity for the clockwise and counter-clockwise rotation for setting 1.6. The red lines mark the rotation.

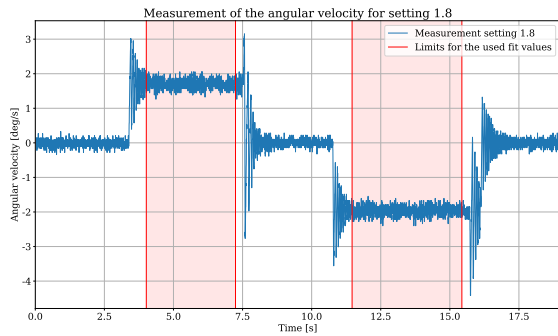


Fig. 19: Measured angular velocity for the clockwise and counter-clockwise rotation for setting 1.8. The red lines mark the rotation.

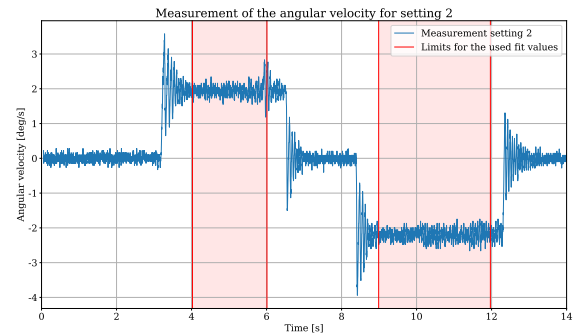


Fig. 20: Measured angular velocity for the clockwise and counter-clockwise rotation for setting 2. The red lines mark the rotation.

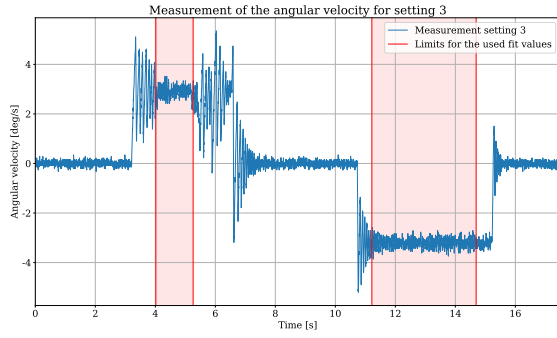


Fig. 21: Measured angular velocity for the clockwise and counter-clockwise rotation for setting 3. The red lines mark the rotation.

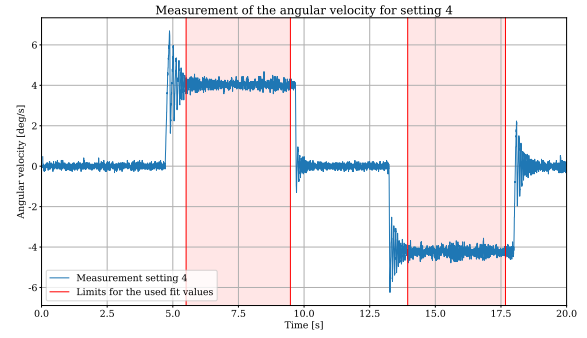


Fig. 22: Measured angular velocity for the clockwise and counter-clockwise rotation for setting 4. The red lines mark the rotation.

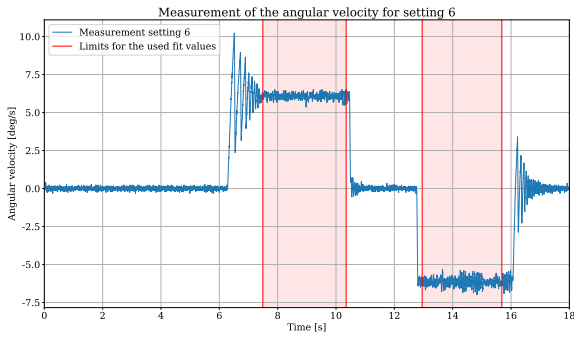


Fig. 23: Measured angular velocity for the clockwise and counter-clockwise rotation for setting 6. The red lines mark the rotation.

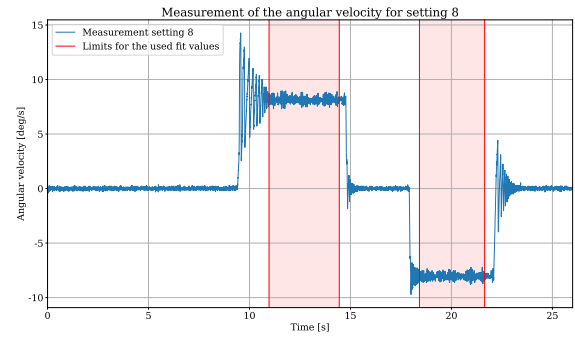


Fig. 24: Measured angular velocity for the clockwise and counter-clockwise rotation for setting 8. The red lines mark the rotation.

7.3 Measurement of the instrument scale factor

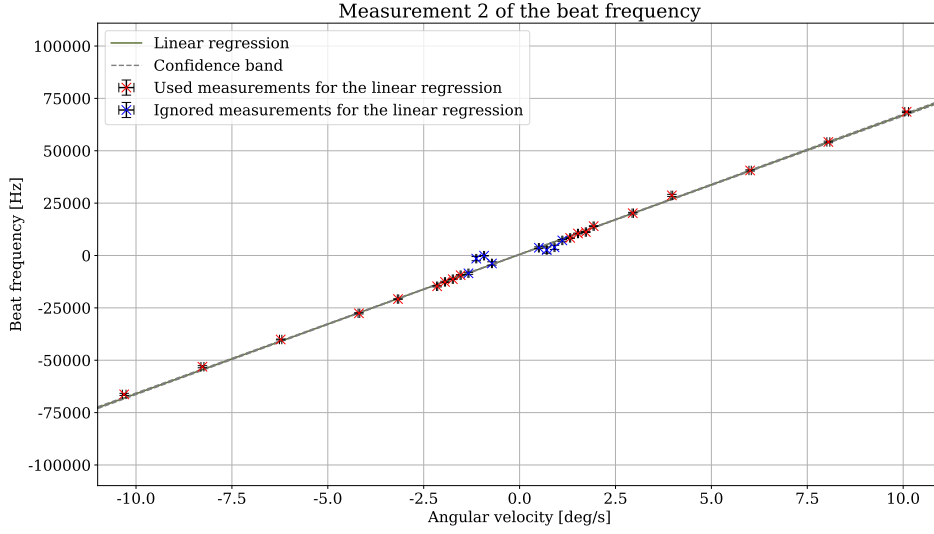


Fig. 25: Second measurement of the beat frequencies. On the y -axis the measured values of the beat frequency f in Hz are plotted against the angular velocities ω_{real} in deg/s. In red all the used values for the regression are plotted, in blue the ignored values are shown. The confidence band is again very small.

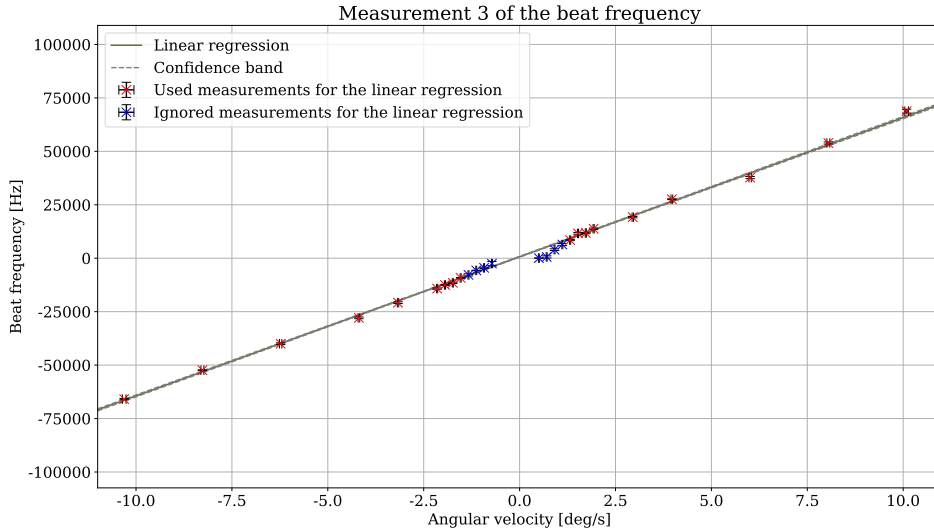


Fig. 26: Third measurement of the beat frequencies. On the y -axis the measured values of the beat frequency f in Hz are plotted against the angular velocities ω_{real} in deg/s. In red all the used values for the regression are plotted, in blue the ignored values are shown. The confidence band is again very small.

7.4 Lab notes

Cuse gyroscope — Lab notes — 27.09.22

a) alignment of cuse — done
 alignment of etalon — turned until
 good signal visible
 alignment of beam splitter — alignment for
 heat measuring setup — heard far point
 + oscilloscope

Screenings:

- 01 — check of signal
- 02 — check of signal with
 realigned etalon
- 03 — speed 0.6 signal check
 CW-rotation
- 04 — //
 CCW-rotation
- 05 — speed 0.3 CW-rotation
- 06 — speed 0.3 CCW-rotation
- 07 — speed 1 CW-rotation
- 08 — speed 1 CCW-rotation
- 09 — speed 4 CW-rotation
- 10 — speed 4 CCW-rotation
- 11 — speed 10 CW-rotation
- 12 — speed 10 CCW-rotation
- 13+ — speed 20 higher resolution

Measurements: until speed of 0.6 gaps in the signal
 possible explanation: below Lock-in angular velocity
 Uncertainty of the measured beat-frequency is estimated
 by assessing the fluctuations

Tube current: 6.5 mA Amplifier gain: 0.1

Fig. 27: Lab notes - page 1

| Speed ω (rad) | rotation direction | beat frequency in Hz |
|----------------------|--------------------------|----------------------|
| 1 | clock-wise (CW) | 4000 \pm 500 |
| 1 | counter-clock-wise (CCW) | 300 \pm 200 |
| 2 | CW | 15.500 \pm 200 |
| 2 | CCW | 17.500 \pm 200 |
| 3 | CW | 20.200 \pm 200 |
| 3 | CCW | 20.400 \pm 400 |
| 4 | CW | 27.400 \pm 200 |
| 4 | CCW | 28.500 \pm 200 |
| 6 | CW | 40.800 \pm 500 |
| 6 | CCW | 40.500 \pm 300 |
| 8 | CW | 56.600 \pm 800 |
| 8 | CCW | 53.000 \pm 600 |
| 10 | CW | 68.500 \pm 300 |
| 10 | CCW | 66.500 \pm 600 |
| 1,8 | CW | 11.800 \pm 200 |
| 1,8 | CCW | 12.000 \pm 200 |
| 1,6 | CW | 10.500 \pm 200 |
| 1,6 | CCW | 11.800 \pm 300 |
| 1,4 | CW | 5.700 \pm 400 |
| 1,4 | CCW | 8.800 \pm 200 |
| 1,2 | CW | 7.200 \pm 600 |
| 1,2 | CCW | 5.000 \pm 1000 |
| 0,8 | CW | 2800 \pm 1000 |
| 0,8 | CCW | 800 \pm 400 |
| 0,6 | CW | 100 \pm 100 |
| 0,6 | CCW | 1800 \pm 400 |
| 0,6 | CW | 3700 \pm 400 |
| 0,6 | CCW | 3800 \pm 800 |
| 0,8 | CW | 7600 \pm 1500 |
| 0,8 | CCW | 100 \pm 100 |
| 1 | CW | 3300 \pm 1000 |
| 1 | CCW | 1500 \pm 1000 |
| 1,2 | CW | 7200 \pm 400 |
| 1,2 | CCW | 8500 \pm 500 |
| 1,4 | CW | 8400 \pm 300 |
| 1,4 | CCW | 9400 \pm 300 |
| 1,6 | CW | 10500 \pm 200 |
| 1,6 | CCW | 11.300 \pm 200 |
| 1,8 | CW | 11.200 \pm 200 |
| 1,8 | CCW | 12.600 \pm 300 |
| 2 | CW | 14.000 \pm 200 |
| 2 | CCW | 16.200 \pm 500 |
| 3 | CW | 20.200 \pm 400 |
| 3 | CCW | 20.800 \pm 100 |
| 4 | CW | 28.200 \pm 500 |
| 4 | CCW | 27.600 \pm 300 |
| 6 | CW | 40.600 \pm 300 |
| 6 | CCW | 40.100 \pm 200 |
| 8 | CW | 54.200 \pm 400 |
| 8 | CCW | 53.100 \pm 500 |
| 10 | CW | 68.600 \pm 300 |
| 10 | CCW | 66.500 \pm 500 |

Fig. 28: Lab notes - page 2

| speed ω (au) | rotation direction | beat frequency [Hz] |
|---------------------|--------------------|---------------------|
| 0,6 | | 60 ± 60 |
| 0,6 | CW | 2500 ± 1000 |
| 0,8 | CCW | 600 ± 500 |
| 0,8 | CW | 4500 ± 300 |
| 1 | CCW | 4000 ± 400 |
| 1 | CW | 5700 ± 100 |
| 1,2 | CCW | 6400 ± 500 |
| 1,2 | CW | 7800 ± 500 |
| 1,4 | CCW | 8500 ± 300 |
| 1,4 | CW | 9200 ± 200 |
| 1,6 | CCW | 11600 ± 400 |
| 1,6 | CW | 11500 ± 300 |
| 1,8 | CCW | 11800 ± 300 |
| 1,8 | CW | 12500 ± 200 |
| 2 | CCW | 13.800 ± 300 |
| 2 | CW | 14.200 ± 300 |
| 3 | CCW | 19.200 ± 300 |
| 3 | CW | 20.800 ± 400 |
| 4 | CCW | 27.600 ± 200 |
| 4 | CW | 22.900 ± 400 |
| 6 | CCW | 37.700 ± 500 |
| 6 | CW | 40.000 ± 400 |
| 8 | CCW | 53.900 ± 500 |
| 8 | CW | 52.400 ± 200 |
| 10 | CCW | 62.800 ± 500 |
| 10 | CW | 65.900 ± 300 |

=) measuring the speed with Phyfox:

10, 8, 6, 4, 3, 2, 1,8, 1,6, 1,4, 1,2, 1

Fig. 29: Lab notes - page 3